

Short Communication

Research on Mechanical Property of CoMo and CoMoP Coatings Electrodeposited on Iron Substrate

Zheng Xiong^{1,*}, Ji Sun², Qiang Wan¹

¹ School of Mechatronics and Automation, Wuchang Shouyi University, Wuhan, China 430070

² School of Materials Science and Engineering, Anhui University of Technology, Maanshan, China 243000

*E-mail: dr_xiong_wcuniver@163.com

Received: 22 April 2022 / Accepted: 26 May 2022 / Published: 4 July 2022

Many mechanical parts, such as mechanical arm requires iron-based materials with optimal mechanical property. In the paper, CoMo coating and CoMoP coating are prepared by electrodeposition on the iron substrate to greatly improve mechanical property. The electrodeposition of cobalt and molybdenum belongs to induced codeposition. It is also found that the deposition of cobalt and phosphorus is an interdependent process. Sodium hypophosphite in the plating solution can accelerate the cobalt electrodeposition and increase the cobalt content in the coating. The CoMo electrodeposited coating has 63.8% cobalt and 36.2% molybdenum while the CoMoP electrodeposited coating consists of 71.4% cobalt, 18.1% molybdenum and 10.5% phosphorus. Both CoMo and CoMoP coating are crystalline structure with Co_3Mo and MoO_2 . The phosphorus distribution in the grain boundary and lattice of the CoMoP coating is beneficial to refine surface particles, increase surface hardness (521.13 $\text{HV}_{0.1}$) and improve wear resistance ($8.42 \times 10^{-3} \text{ mm}^3$ wear volume).

Keywords: CoMo coating; CoMoP coating; Electrodeposition; Mechanical property;

1. INTRODUCTION

Iron-based materials are considered as a kind of common and fundamental metal materials, which are mainly used in many fields, such as the construction industry, mechanical devices, electronic industry, etc [1-4]. Especially, some mechanical parts require iron-based materials with optimal mechanical property. For example, mechanical arm is a kind of common mechanical part of mechanical industry. The iron-based materials that constitute the mechanical arm need to have better hardness and excellent wear resistance. In order to further meet the needs of the mechanical field, it is necessary to use surface treatment technology to prepare metal alloy coatings on the surface of iron-based materials, so as to greatly improve the mechanical properties of iron-based materials [5-8].

Cobalt is a lustrous steel-gray metal with a melting point of 1493°C, which is hard and considered as an important raw material for the production of hard alloys. Moreover, molybdenum is a silver-white metal which is also hard and tough with a high melting point. It is found that the CoMo alloy has excellent mechanical property with better hardness and good wear resistance. Many researchers have prepared CoMo alloy coating by physical and chemical methods [9-13]. In addition, in order to further improve the mechanical property of CoMo alloy coating, some nano-particles are added to prepare CoMo composite coating. It is reported that nano-particles such as ZrO₂, Al₂O₃, SiC, etc can greatly improve the mechanical property of CoMo alloy coatings on the surface of materials [14-16]. In fact, in addition to nano-particles, adding non-metallic elements in metal alloys is also beneficial to improve the mechanical properties of metal alloys. For example, phosphorus has a strong solid solution strengthening, which can effectively improve the strength and hardness of materials [17-18]. Due to the use of sodium hypophosphite as reductant in electroless deposition, the effect of phosphorus on the properties of alloy coatings in the process of electroless plating has been reported in many literatures [19-20]. In the paper, the CoMo and CoMoP coating is prepared on iron substrate respectively from solutions with and without sodium hypophosphite by electrodeposition. The mechanical property of iron substrate, CoMo coating and CoMoP coating is studied.

2. EXPERIMENTAL

2.1 Solution and technological parameters

The solution composition of the CoMo and CoMoP electrodeposited coating is listed in Table 1.

Table 1. Composition of plating solution for CoMo and CoMoP coating

Chemical agent	Concentration(g/L)	
	CoMo coating	CoMoP coating
Cobalt sulfate	20	20
Sodium molybdate	10	10
Sodium hypophosphite	-	10
Sodium sulfate	15	15
Ammonium citrate	60	60
Boric acid	35	35

The cobalt sulfate and sodium molybdate provide cobalt and molybdate ions respectively for CoMo electrodeposition. The phosphorus in the CoMoP coating derives from sodium hypophosphite. Sodium sulfate is used as conducting salt to improve electrodeposition efficiency. Moreover, ammonium citrate is chosen as the complexing agent while boric acid is as the buffering agent. The pH value of the solution is adjusted to 7 using sodium hydroxide. The CoMo coating and CoMoP coating

is obtained from the solution with and without sodium hypophosphite using the current density 2 A/dm² for 60 min at 60 °C.

2.2. Experimental process and testing

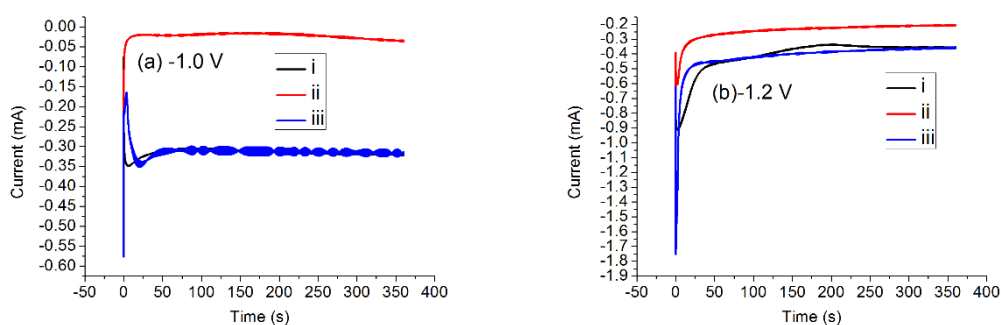
The surface area of pure iron sheet as the substrate is 4 cm² (2 cm×2 cm) while the graphite sheet as counter electrode is 9 cm² (3 cm×3 cm). The area of the counter electrode is twice that of the working electrode to ensure a more uniform current distribution on the substrate. The surface pretreatment of iron substrate before plating is as follows: polishing → pure water cleaning → alkaline wash (40 g/L sodium carbonate and 10 g/L sodium hydroxide) at 50 °C for 10 min → pure water cleaning → acid pickling (15% hydrochloric acid) at 30 °C for 1 min → pure water cleaning → drying → electrodeposition of CoMo and CoMoP coating. After the electrodeposition is finished, the sample is dried and tested.

The chronoamperometry of Co, CoMo and CoMoP electrodeposited at different potentials is studied by electrochemical station (Iviumstat) to analyze the codeposition of CoMo and CoMoP coatings. The potential is selected as -1.0 V, -1.2 V and -1.4 V respectively for 360 s at 60 °C. The surface morphology of samples is observed by scanning electronic microscope (Hitachi TM4000) while the surface element distribution of sample is analyzed by energy disperse spectroscopy (EDX4500H). X-Ray diffraction (DX2700) is used to characterize the structure of coatings at 2°/s scanning rate from 30° to 70°. The hardness of the coatings is tested by digital Vickers hardness tester (HV-1000) at 0.98 N with 15 s holding time. The mechanical property of coatings is evaluated by friction and wear testing machine (ZMM30) and scratch tester (WS292) based on the wear scar and scratch on the sample surface. The surface profiler (Tencor P7) is used to describe the 3D morphology of wear scar.

3. RESULT AND DISCUSSION

3.1 Chronoamperometry and surface morphology of CoMo and CoMoP electrodeposition

The chronoamperometry of Co, CoMo and CoMoP electrodeposited at -1.0 V, -1.2 V and -1.4 V on iron substrate for 360 s at 60 °C is seen in figure 1.



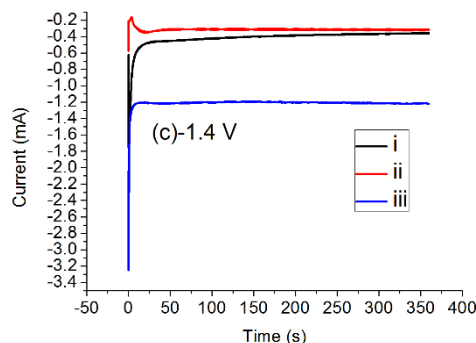
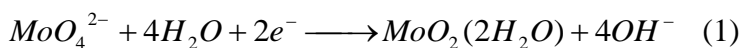


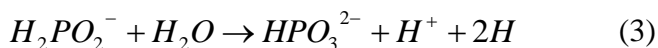
Figure 1. Chronoamperometry of Co, CoMo and CoMoP electrodeposition at -1.0 V, -1.2 V and -1.4 V for 360 s at 60 °C. i: 0.01 mol/L CoSO₄; ii: 0.01 mol/L CoSO₄+0.01 mol/L Na₂MoO₄; iii: 0.01 mol/L CoSO₄+0.01 mol/L Na₂MoO₄+0.01 mol/L NaH₂PO₂;

According to figure 1, the deposition current of Co, CoMo and CoMoP at same deposition potential is totally different. The relationship between time and current is useful to analyze the nucleation mechanism and codeposition process for metal ions. Generally speaking, the deposition current decreases gradually due to double layer charging during the initial period of electrodeposition. With the increase of electrodeposition time, the deposition current increases gradually and reaches the maximum value due to the nucleation and growth of metal which increase the surface area and the surface current distribution, resulting in the increase of deposition current. As the electrodeposition goes on, the thickness of diffusion layers increases and the deposition current decreases gradually. When the system reaches a chemical equilibrium, the deposition current tends to be stable. According to the data in figure 1, when the electrochemical equilibrium is reached, the deposition current of CoMo is the smallest while the deposition current of CoMoP is the largest, and the deposition current of Co is between that of CoMo and CoMoP.

It can be seen that the addition of sodium molybdate in the plating solution prevents the electrodeposition of cobalt. The codeposition of cobalt and molybdenum belongs to induced codeposition. Molybdenum cannot be electrodeposited directly from aqueous solution alone, but codeposition of cobalt and molybdenum can be induced by autocatalysis on cobalt surface to form CoMo alloy coating. The codeposition mechanism of cobalt and molybdenum is reported by the following equations [21].



The electrodeposition current of CoMoP coating is the largest which indicates that adding sodium hypophosphite in the solution accelerates the electrodeposition of cobalt. The precipitation of phosphorus can be explained in the following equations [22-23].



The primary hydrogen decomposed by hypophosphite is adsorbed on the surface of cobalt metal, which catalyzes the primary hydrogen and promotes the phosphorus precipitation. The deposition of cobalt and phosphorus is an interdependent process. The electrodeposited cobalt acts as the surface catalytic center to promote the precipitation of phosphorus while the precipitation of phosphorus in turn promotes the deposition of cobalt [24].

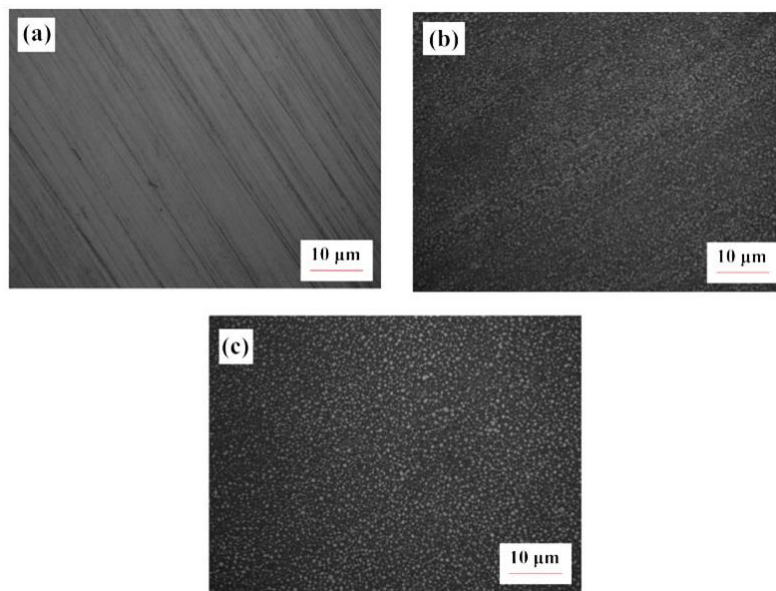


Figure 2. The surface morphology of iron substrate, CoMo coating and CoMoP coating. a: iron substrate; b: CoMo coating; c: CoMoP coating; The accelerating voltage is 15 kV.

The surface morphology of the iron substrate is relatively flat after pretreatment, and some polished scratches can be observed. The surfaces of both CoMo and CoMoP coatings are composed of granular structures. The surface porosity of the CoMo coating is large, the particle size is not uniform, and some scratches can be observed on the surface. The addition of sodium molybdate in the solution hinders the electrodeposition process of cobalt, which reduces the deposition rate. The surface morphology of the CoMoP coating is very dense and the particle size is uniform. On one hand, the phosphorus promotes the electrodeposition of cobalt, which increases the deposition rate. On the other hand, phosphorus can enter the grain boundary and lattice of CoMo alloy coating that play the role of refining surface particles.

3.2 Structure and composition of CoMo and CoMoP coating

The XRD pattern of CoMo and CoMoP electrodeposited coating is shown in figure 3. Five obvious diffraction peaks could be observed based on the XRD patterns which mean that the electrodeposited CoMo and CoMoP coating are crystalline structure. The three strong diffraction peaks (a, b and c) indicate the structure of Co_3Mo which is a typical tetrahedron structure [25]. The two diffraction peaks with lower intensity (d and e) are the diffraction peaks of MoO_2 . Compared with

CoMoP, the diffraction peak intensity of molybdenum oxide in CoMo coating is stronger, which is attributed to the codeposition process induced by cobalt and molybdenum [26-27]. The molybdate ions gain electrons to form molybdenum oxide. It can be seen from the previous analysis that phosphorus and cobalt have a synergy effect. The addition of sodium hypophosphite to the plating solution is beneficial to increase the content of cobalt in the coating, which increases the diffraction intensity of Co_3Mo and reduces the diffraction peak intensity of molybdenum oxide.

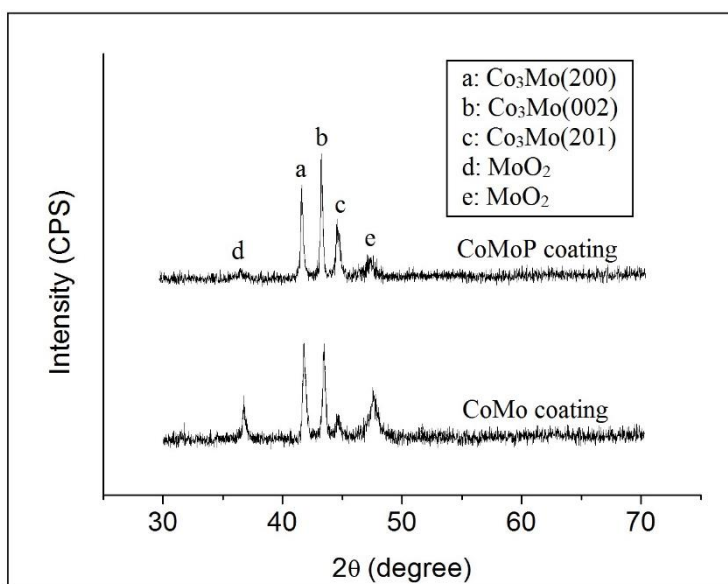


Figure 3. XRD patterns of CoMo and CoMoP coating. The scanning rate is $2^\circ/\text{s}$ from 30° to 70° .

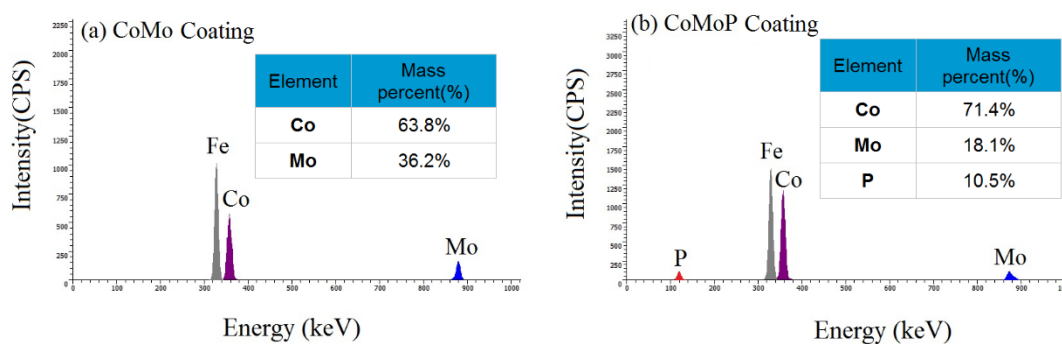


Figure 4. EDS pattern of CoM and CoMP coating. The energy resolution is 150 eV.

The CoMo electrodeposited coating possesses 63.8% cobalt and 36.2% molybdenum. The molybdenum in the coating originates from the Co_3Mo structure and MoO_2 . The CoMoP electrodeposited coating is composed of 71.4% cobalt, 18.1% molybdenum and 10.5% phosphorus. The sodium hypophosphite in the plating solution is beneficial to increase the cobalt and phosphorus content in the CoMoP coating, but decrease the amounts of molybdenum.

3.3 Hardness and scratch resistance of CoMo and CoMoP coating

The Vickers hardness tester is used to apply a pressure of 0.98 N on the surface of the sample and hold it for 15 seconds to calculate the hardness value of the sample according to the area of the indentation. The results are shown in figure 5 and table 2. The indentation of the iron substrate is the largest while the indentation of the CoMoP coating is the smallest, and the indentation of the CoMo coating is between that of the iron substrate and CoMoP coating. According to the data in table 2, the Vickers hardness of the iron substrate is the smallest about 163.78 HV_{0.1}. The Vickers hardness of the CoMo coating is 323.54 HV_{0.1} while the hardness of the CoMoP coating is the highest, reaching 521.13 HV. It is known that Co₃Mo has a stable tetrahedral structure, and the hardness and melting point of cobalt and molybdenum are very high, so the hardness of CoMo coating electrodeposited on iron substrate is greatly improved compared to the iron substrate. The addition of phosphorus is beneficial to refine the surface particles of the CoMoP coating, increase the content of cobalt, and further improve the hardness. The effect of phosphorus on the grain size of alloys has been investigated in some literatures so far [28-29].

Table 2. The hardness of iron substrate, CoMo and CoMoP coating based on rhomb indentation

Samples	D ₁ (μm)	D ₂ (μm)	HV _{0.1}
Iron substrate	33.12	34.86	163.78
CoMo coating	23.73	24.63	323.54
CoMoP coating	18.98	19.12	521.13

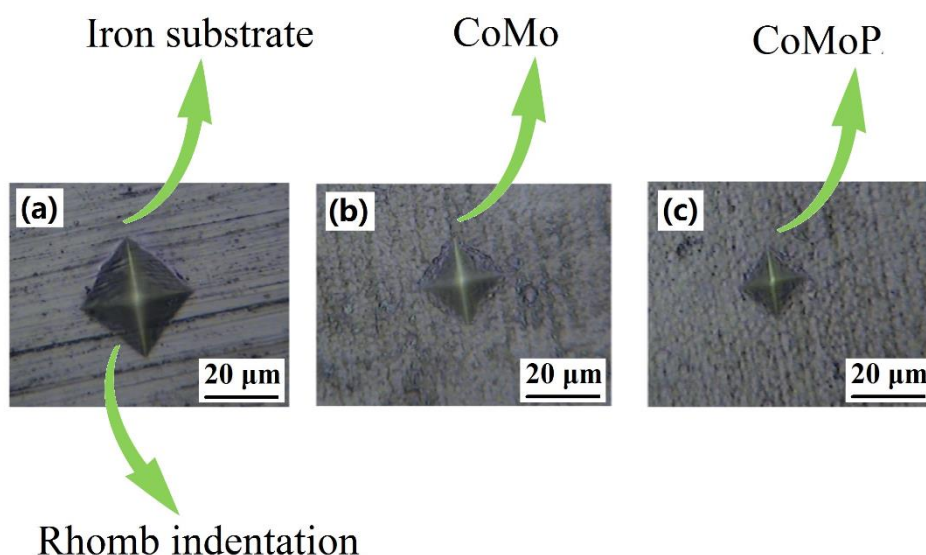


Figure 5. Vickers hardness of iron substrate, CoMo coating and CoMoP coating. The loading force is 0.98 N with 15 s holding time.

Figure 6 shows the variation trend of the friction force on the surface of the sample and the surface morphology of the scratches. When the loading force on the sample surface gradually increases

from 0 N to 90 N, the frictional force on the sample surface also increases accordingly. When the load is 90 N, the friction forces of the iron substrate, CoMo coating and CoMoP coating are 1200 g, 1120 g and 880 g, respectively. According to the scratch morphology, when the load is relatively small, the scratches are finer. With the gradual increase of the loading force, the scratches on the sample surface gradually thicken. When the load is 90 N, the scratch width of the iron substrate is the largest, and the scratch width of the CoMoP coating is the smallest. It can be seen that the scratch resistance of CoMoP coating is the best compared to iron substrate and CoMo coating. The main reason is that the addition of phosphorus increases the cobalt content in the coating and at the same time refines the surface particles of the coating, which reduces the surface porosity of the coating, increases the compactness, and greatly improves the mechanical properties of the coating.

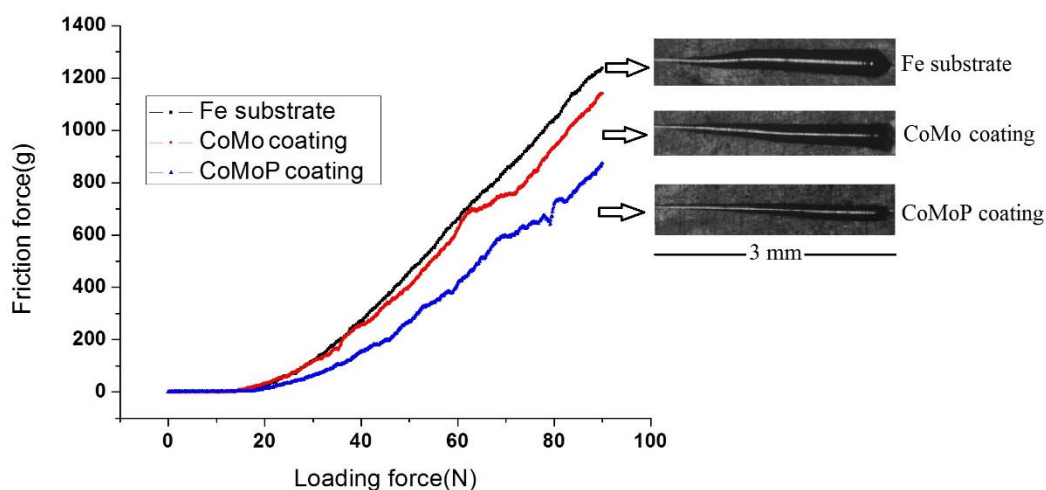


Figure 6. Friction force and scratch morphology of samples. The loading force is increased from 0 N to 90 N.

3.4 Wear resistance of CoMo and CoMoP coating

The top views of wear scars on samples are illustrated in figure 7. The wear scar depth can directly evaluate the wear resistance of the sample. According to the depth ruler, the surface depth gradually increases as the color changes from white to black. The wear scar on the iron substrate shows a continuous dark black in the middle, indicating that the wear scar is very deep. It can be seen from the top view of the CoMo coating that there is a small amount of black area in the middle, indicating that some areas of the wear scar are deeper. According to figure 7(c), most areas on the wear scars of the CoMoP coating show red color, indicating that the depth of the wear scars is shallow. Comparing the three top views, it can be found that the CoMoP coating has the shallowest wear scar and the best wear resistance, which is consistent with the previous analysis results.

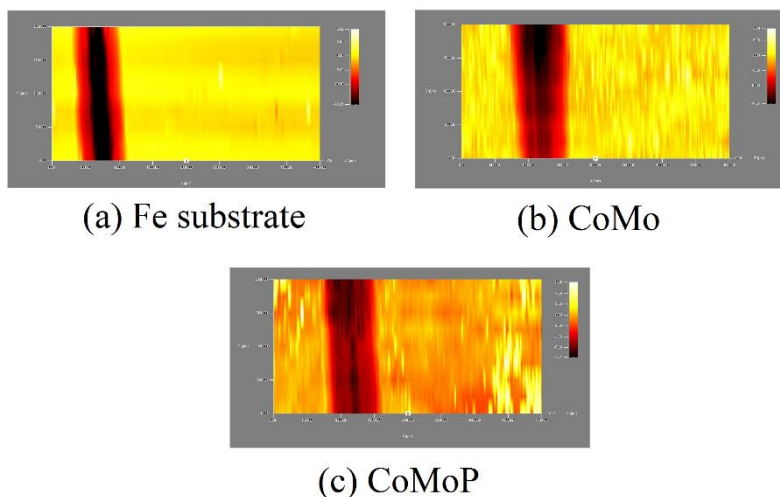


Figure 7. Top views of wear scars on iron substrate, CoMo coating and CoMoP coating after reciprocating friction with 10 N loading force for 30 min.

In order to better calculate the depth, cross-sectional area and volume of the wear scar, the surface profiler is used to scan the wear scar from left to right to draw a 3D graph of the wear scar, as shown in figure 8 and table 3.

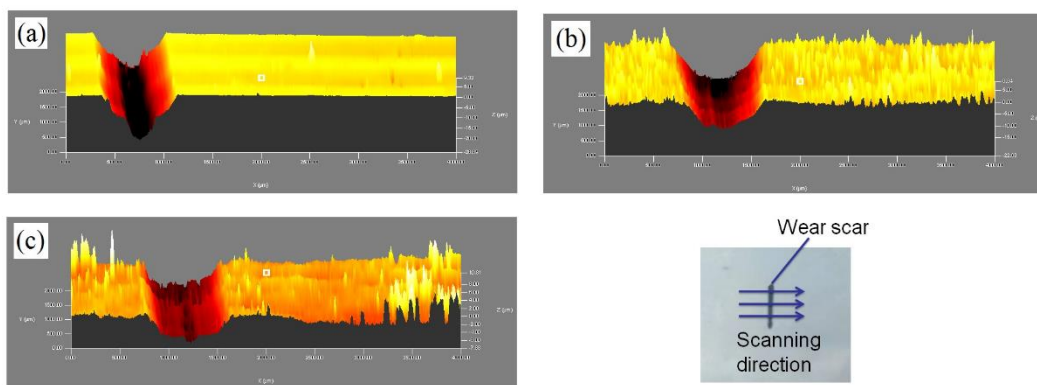


Figure 8. 3D morphology of wear scar on iron substrate, CoMo coating and CoMoP coating.

Table 3. Geometrical parameters of wear scar on iron substrate, CoMo coating and CoMoP coating.

Samples	Maximum depth of wear scar (μm)	Cross-sectional area of wear scar (μm^2)	Volume of wear scar (mm^3)
Iron substrate	17.25	10176.23	20.35×10^{-3}
CoMo coating	14.07	7410.35	14.82×10^{-3}
CoMoP coating	7.81	4213.92	8.42×10^{-3}

Regarding to the data of table 3, it is conspicuous that the iron substrate has the largest wear scar depth (17.25 μm) and maximum wear volume ($20.35 \times 10^{-3} \text{ mm}^3$) showing poor wear resistance. Compared with iron substrate, CoMo coating has better wear resistance property with wear scar depth (14.07 μm) and wear volume ($14.82 \times 10^{-3} \text{ mm}^3$). Furthermore, the CoMoP electrodeposited coating possesses the smallest wear scar depth (7.81 μm) and the minimum wear volume ($8.42 \times 10^{-3} \text{ mm}^3$) indicating the best wear resistance property. Some people also report that the phosphorus element in the alloys can refine the grain size and affect the mechanical property of alloys [30-31].

4. CONCLUSION

CoMo coating and CoMoP coating are prepared by electrodeposition on the iron substrate. Composition, surface morphology, structure and mechanical properties of CoMo coating and CoMoP coating are investigated and analyzed. The conclusions are as follows.

(1) The codeposition of cobalt and molybdenum can be induced by autocatalysis on cobalt surface to form CoMo alloy coating which is considered as induced codeposition. Adding sodium hypophosphite in the solution accelerates the electrodeposition of cobalt to obtain CoMoP coating. The surfaces of both CoMo and CoMoP coatings are composed of granular structures. However, CoMoP coating has more compact and denser surface morphology due to the effect of phosphorus.

(2) The CoMo electrodeposited coating possesses 63.8% cobalt and 36.2% molybdenum while the CoMoP electrodeposited coating is composed of 71.4% cobalt, 18.1% molybdenum and 10.5% phosphorus. The CoMo and CoMoP coating are both crystalline with Co_3Mo tetrahedron structure. It is found out that the addition of phosphorus is beneficial to refine the surface particles of the CoMoP coating, increase the content of cobalt, and further improve the mechanical property. The CoMoP electrodeposited coating has the largest hardness (521.13 $\text{HV}_{0.1}$) and the smallest wear volume which is only $8.42 \times 10^{-3} \text{ mm}^3$.

ACKNOWLEDGEMENT

This research is supported by doctoral research start-up fund of Wuchang Shouyi University (No.0851907).

References

1. V. Mymrin, D. E. Pedroso, C. L. Pedroso, M. A. Avanci, P. H. B. Rolim, K. Q. Carvalho and R. E. Catai, *Constr. Build. Mater.*, 298 (2021) 123698.
2. Y. L. Yuan, X. N. Guo, X. P. He, B. Zhang and S. G. Liu, *Biotechnol. Lett.*, 26 (2004) 311.
3. I. V. Egiz and V. F. Shamrai, *Met. Sci. Heat Treat.*, 43 (2001) 51.
4. E. N. Fedoseeva, V. F. Zanozina, A. D. Zorin and L. E. Samsonova, *Metall.*, 59 (2015) 374.
5. K. Zhan, Y. L. Zhang, L. Bao, Z. Yang, B. Zhao and V. Ji, *Surf. Coat. Technol.*, 423 (2021) 127589.
6. V. Witzl, A. C. Rovani, G. Pintaude, M. S. F. Lima, W. L. Guesser and P. C. Borges, *Tribol. Int.*, 143 (2020) 106081.
7. Z. A. A. Halim, N. Ahmad, M. F. Hanapi and M. N. F. Zainal, *Mater. Chem. Phys.*, 260 (2021) 124134.
8. H. Y. Du, Y. L. An, Y. H. Wei, X. D. Liu, L. F. Hou, B. S. Liu, M. M. Liu and P. K. Liaw, *Mater.*

- Sci. Eng., A*, 744 (2019) 471.
9. C. D. G. Esparza, J. C. Cisneros, I. E. Guel, J. G. C. Morena, J. M. H. Ramirez and R. M. Sanchez, *J. Alloys Compd.*, 615 (2014) S638.
 10. H. Cesiulis, N. Tsyntaru, A. Budreika and N. Skridaila, *Surf. Eng. Appl. Electrochem.*, 46 (2010) 406.
 11. Z. A. Hamid, A. A. Aal, A. Shaaban and H. B. Hassan, *Surf. Coat. Technol.*, 203 (2009) 3692.
 12. V. V. Kuznetsov, Y. Gambur, V. V. Zhulikov, V. M. Krutskikh, E. A. Filatova, A. L. Trigub and O. A. Belyakova, *Electrochim. Acta*, 354 (2020) 136610.
 13. T. Katayama, S. Mo, Y. J. Kurauchi, A. Chikamatsu and T. Hasegawa, *Thin Solid Films*, 728 (2021) 138696.
 14. M. A. Kazakova, Y. V. Vatutina, I. P. Prosvirin, E. Y. Gerasimov, A. V. Shuvaev, O. V. Klimov, A. S. Noskov and M. O. Kazakov, *Microporous Mesoporous Mater.*, 317 (2021) 111008.
 15. D. Nicosia and R. Prins, *J. Catal.*, 229 (2005) 424.
 16. R. Aravind, G. S. Brahma, A. K. Sahu and T. Swain, *Mater. Today Proc.*, 46 (2021) 8586.
 17. K. G. Keong, W. Sha and S. Malinov, *Surf. Coat. Technol.*, 168 (2003) 263.
 18. X. B. Xi, R. H. Zhang and F. H. Sun, *Diamond Relat. Mater.*, 74 (2017) 164.
 19. T. M. Reis, C. D. Boeira, F. L. Serafini, M. C. M. Farias, C. A. Figueroa and A. F. Michels, *Surf. Coat. Technol.*, 438 (2022) 128374.
 20. D. R. Dhakal, Y. K. Kshetri, G. Gyawali, T. H. Kim, J. H. Choi and S. W. Lee, *Appl. Surf. Sci.*, 541 (2021) 148403.
 21. V. S. Kublanovsky and Y. S. Yapontseva, *Electrocatalysis*, 5 (2014) 372.
 22. Y. C. Wu, Z. Y. Zhang, K. Xu, J. Z. Lu, A. Wang, X. R. Dai and H. Zhu, *Appl. Surf. Sci.*, 535 (2021) 147707.
 23. K. Dhanapal, V. Narayanan and A. Stephen, *Mater. Chem. Phys.*, 166 (2015) 153.
 24. S. P. S. Nikova, A. I. Dikumar, N. I. Tsyntaru and J. P. Celis, *Surf. Eng. Appl. Electrochem.*, 44 (2008) 428.
 25. S. Costovici, A. C. Manea, T. Visan and L. Anicai, *Electrochim. Acta*, 207 (2016) 97.
 26. M. C. Esteves, P. T. A. Sumodjo and E. J. Podlaha, *Electrochim. Acta*, 56 (2011) 9082.
 27. Y. Messaoudi, N. Fenineche, A. Guittoum, A. Azizi, G. Schmerber and A. Dinia, *J. Mater. Sci.: Mater. Electron.*, 24 (2013) 2962.
 28. S. Zhang, X. Xin, L. X. Yu, A. Zhang, W. R. Sun and X. F. Sun, *Metall. Mater. Trans. A*, 47 (2016) 4092.
 29. L. H. Li and S. Tin, *J. Alloys Compd.*, 829 (2020) 154352.
 30. M. Q. Wang, J. H. Du, Q. Deng, Z. L. Tian and J. Zhu, *Mater. Sci. Eng. A*, 626 (2015) 382.
 31. S. L. Yang, W. R. Sun, J. X. Wang, Z. M. Ge, S. R. Guo and Z. Q. Hu, *J. Mater. Sci. Technol.*, 27 (2011) 539.